Effect of Charge Substitutions at Residue His-142 on Voltage Gating of Connexin43 Channels

Junko Shibayama,* Cristina Gutiérrez,† Daniel González,† Fabien Kieken,‡ Akiko Seki,§ Jesus Requena Carrión,¶ Paul L. Sorgen,‡ Steven M. Taffet,‖ Luis C. Barrio,† and Mario Delmar*

*Department of Pharmacology, State University of New York Upstate Medical University, Syracuse, New York; †Department of Biochemistry and Molecular Biology, University of Nebraska Medical Center, Omaha, Nebraska; ‡Unit of Experimental Neurology, Research Department, ''Ramón y Cajal'' Hospital, Madrid, Spain; §Department of Cardiology, Tokyo Women's Medical University, Tokyo, Japan; ¶Departamento de Teoría de la Señal y Comunicaciones, Universidad Carlos III de Madrid, Madrid, Spain; and ‖Microbiology/Immunology, State University of New York Upstate Medical University, Syracuse, New York

ABSTRACT Previous studies indicate that the carboxyl terminal of connexin43 (Cx43CT) is involved in fast transjunctional voltage gating. Separate studies support the notion of an intramolecular association between Cx43CT and a region of the cytoplasmic loop (amino acids 119–144; referred to as "L2"). Structural analysis of L2 shows two α-helical domains, each with a histidine residue in its sequence (H126 and H142). Here, we determined the effect of H142 replacement by lysine, alanine, and glutamate on the voltage gating of Cx43 channels. Mutation H142E led to a significant reduction in the frequency of occurrence of the residual state and a prolongation of dwell open time. Macroscopically, there was a large reduction in the fast component of voltage gating. These results resembled those observed for a mutant lacking the carboxyl terminal (CT) domain. NMR experiments showed that mutation H142E significantly decreased the Cx43CT-L2 interaction and disrupted the secondary structure of L2. Overall, our data support the hypothesis that fast voltage gating involves an intramolecular particle-receptor interaction between CT and L2. Some of the structural constrains of fast voltage gating may be shared with those involved in the chemical gating of Cx43.

INTRODUCTION

Gap junction channels form a low-resistive pathway for the passage of ions and small molecules between cells. These channels are formed by oligomerization of a protein called connexin. Each connexin subunit crosses the cell membrane four times, thus yielding three intracellular domains: the amino terminal (NT), the carboxyl terminal (CT), and a cytoplasmic loop (CL) that spans from the second to the third transmembrane domains. The most abundant connexin molecule in the heart is the 43-kD isotype, connexin43 (Cx43). It is generally accepted that the CT region of Cx43 acts as a regulatory domain. Like many other channel proteins, the conducting properties of these channels can be regulated both by chemical factors (1,2) as well as by voltage (3,4). In this manuscript, we characterize the molecular mechanisms mediating voltage gating of Cx43.

A voltage gradient applied between two Cx43-expressing cells (V_j) leads to a corresponding flow of current across gap junctions (I_j). Like most membrane channels, gap junctions show voltage-dependent gating behavior. For V_j values $>\sim$40 mV, junctional currents inactivate with a time course that is best described by two time constants (''fast'' and ''slow''; see (3,4)). At the single channel level, the fast exponential component corresponds to the voltage-dependent fast transitions between the open and the ''residual'' state (4,5). In turn, the presence of a residual state explains the fact that macroscopic junctional currents do not inactivate completely (i.e., junctional current does not reach zero for a long pulse (4)). Previous studies have shown that truncation of the Cx43CT domain eliminates fast voltage gating (3). Additional studies showed the corresponding loss of the residual state upon CT truncation (4). Coexpression of the CT domain with the truncated channel restored the residual conductive state (4), supporting the idea that during fast voltage gating, the CT may act as a gating particle that interacts with a separate region of the protein (a ''receptor'').

The location of the receptor within the primary sequence of Cx43 remained elusive for some time. Recently, we showed that the CT domain binds in vitro to a synthetic peptide with a sequence corresponding to amino acids 119–144 of Cx43 (i.e., the second half of CL, ''L2''; see (6)). Structural analysis showed that the L2 peptide is conformed as two α-helical domains separated by a poorly defined center region (6). Single channel analysis revealed that the same peptide, when presented in the patch pipette, interfered with the occurrence of the residual state (7). These results led to the suggestion that the L2 region of CL may represent the receptor for the gating particle. However, further assessment of this hypothesis using sequential deletions within the actual Cx43 protein was complicated by the fact that modifications in the CL region were associated with nonfunctional channels (8). Here, we have chosen to modify the primary sequence by site-directed substitutions in amino acid H142, which is contained within the predicted regions of α-helicity (6). Using a combination of voltage clamp, patch clamp, and

Submitted March 24, 2006, and accepted for publication August 16, 2006.

Address reprint requests to Mario Delmar, Dept. of Pharmacology, State University of New York Upstate Medical University, 766 Irving Ave., Syracuse, New York 13210. Tel.: 315-464-7987; Fax: 315-464-8014; E-mail: delmarm@upstate.edu.

0006-3495/06/12/4054/10 $2.00

doi: 10.1529/biophysj.106.085787

NMR, we demonstrate that mutation H142E (histidine replaced by glutamate) has a functional consequence on fast voltage gating comparable to that of CT truncation; in addition, this mutation severely disrupts the integrity of the secondary structure of L2 and drastically interferes with L2-CT binding. Altogether, the data are consistent with the hypothesis that an intramolecular interaction between the CT domain and the L2 region is an essential component of fast voltage gating. These results add to the elucidation of the molecular basis of gating in gap junction channels.

MATERIAL AND METHODS

Site-directed mutagenesis

A variety of histidine mutant constructs were tested in this study. Mutagenesis was carried out using the Quick Change Kit (Stratagene, La Jolla, CA). All sequences were confirmed at the DNA sequencing facility at SUNY-Syracuse.

Dual voltage clamp in *Xenopus* oocytes

Oocytes from *Xenopus laevis* were prepared as described (3). The in vitro transcribed cRNA of Cx43WT or histidine mutants (0.5–1.0 μg/μl, 50 nl/oocyte) was injected in combination with an antisense oligonucleotide directed against *Xenopus* Cx38 mRNA (15 ng/oocyte) to block endogenous expression (9). After removing the vitelline membrane, the oocytes were placed in contact to allow the formation of intercellular channels. Macroscopic junctional current (I_j) flowing between paired oocytes was measured using the dual two-electrode voltage clamp technique as previously described (9). Data acquisition and analysis were performed using pCLAMP. The time courses of I_j transitions were fitted to exponential relations with $R < 0.999$ using Clampfit (pCLAMP). The time course of decay of the junctional current was best described by the sum of two exponentials:

$$I_j = A_{fast}\, e^{-t/\tau 1} + A_{slow}\, e^{-t/\tau 2} + A_r,$$

where the constants A_{fast} and A_{slow} represent the amplitude of the junctional current contributed by the fast and slow components, respectively, at time = 0 and A_r is the steady-state value of current at time = 30 s. To evaluate transjunctional voltage dependence of gap junctions, the junctional conductance steady-state values (G_{jss}) obtained by using pulses of 30-s duration were normalized relative to the conductance value for brief V_j prepulses (10 mV). The averaged G_{jss}/V_j relationship for each polarity of V_j, based on the assumption that each polarity of V_j affected a single gap junction hemichannel, was fit to a Boltzmann relation of the form (10) $G_{jss} = \{(G_{jmax} - G_{jmin})/(1 + \exp[A(V_j - V_o)])\} + G_{jmin}$, which applies to a two-state system with the energy difference between states linearly dependent on voltage. Although not all channels may meet these assumptions (see Results), this analysis still provides useful parameters for comparing the behavior of mutant channels versus wild-type. The G_{jmax} is the maximal conductance, G_{jmin} is the residual conductance at large V_j, V_o is the transjunctional voltage at which $G_{jss} = (G_{jmax} - G_{jmin})/2$, and A ($A = nq/kT$) is a constant that expresses the voltage sensitivity. Fits were made by treating G_{jmax}, G_{jmin}, A, and V_o as free parameters. Constants were estimated from an iterative minimization (least-squares) of the difference between the data and the calculated fit point (SigmaPlot; Jandel Scientific, Chicago, IL). Student's t-test ($P < 0.05$) was used for statistical analysis.

Dual patch clamp

Patch clamp experiments were conducted in communication-deficient murine neuroblastoma cells (N2a) transiently transfected with cDNA for Cx43WT or the corresponding histidine mutants (0.25 μg of internal ribosome entry site plasmid DNA coding eGFP; Quiagen, Valencia, CA). The cells were cultured in Dulbecco's modified Eagle's medium with 10% fetal bovine serum (7). For recording of Cx43 channels, cells were placed on the stage of an inverted microscope equipped for epifluorescence (Nikon Diaphoto200, filter: 520–560 nm; Nikon, Tokyo, Japan). eGFP-positive cell pairs were visualized by the emitted fluorescence (520–560 nm) after excitation with monochromatic light (495 nm) and targeted for electrophysiological analysis. The dual whole-cell voltage clamp technique was used to record gap junction currents. Both cells in the pair (cell1 and cell2) were independently voltage clamped at the same holding potential (−40 mV). The prejunctional cell (cell1) was stepped to +20 mV, creating a potential difference across the junction (V_j) of +60 mV during repetitive 10−30-s steps. Patch pipettes were filled with a solution containing cesium (in mM: 130 CsCl; 0.5 $CaCl_2$; 10 HEPES; 10 EGTA; 2.0 Na_2ATP; 3.0 MgATP; pH 7.2).

Pipette resistance was 3.0−5.0 MΩ. During recording, cells were kept at room temperature in a cesium-containing solution (in mM: 160 NaCl; 10 CsCl; 2.0 $CaCl_2$; 0.6 $MgCl_2$; 10 HEPES; pH 7.4). Octanol was used to decrease macroscopic conductance and resolve single channel events. The concentration of octanol was titrated during the experiment (maximum, 2.0 mM) to maintain a level of uncoupling where only one or two channels remained active. Unitary currents were filtered at 0.1 kHz (−3 db, four-pole Bessel filter, LPF202; Warner Instrument, Hamden, CT) and digitally sampled at 2 kHz (7). Traces of junctional currents were acquired and analyzed using the Clampex software (pClamp version 8.0, Axon Instruments, Union City, CA). Single channel events were manually measured to determine unitary conductance (driving force = +60 mV) and open time. Only events within a range of 25 pA from the baseline that lasted 20 ms or more (to reduce filtering artifacts) were included in the events histogram. All single channel data (open times as well as conductance values) were obtained from traces where only one or, at the most, two channels were active. This allowed us to define a nonconductive (''closed'') state by the absence of junctional current in the presence of a voltage gradient. In turn, the level at which $I_j = 0$ was defined by the level of holding current delivered by the second amplifier when $V_j = 0$. Histograms were constructed using Origin (version 7.0; Microcal, Northampton, MA).

Production of recombinant protein

Recombinant Cx43CT was produced as previously described (6). Briefly, cDNA derived from rat Cx43 was inserted into pGEX-6P-2 (Amersham, Buckinghamshire, UK) and expressed in *Escherichia coli* (BL-21). The resultant GST-fusion protein was cleaved from the glutathione-S-transferase (GST) PreScission Protease (Amersham Biosciences). The recombinant product after cleavage from GST contained the sequence 255–382 of rCx43 preceded by four additional amino acids (GPLG). Protein concentration was measured using the Bio-Rad (Hercules, CA) DC Protein Assay. Protein purity was assessed by sodium dodecyl sulfate-polyacrylamide gel electrophoresis.

NMR spectroscopy

NMR experiments (two-dimensional proton ^2H double quantum-filtered (DQF)-correlation spectroscopy (COSY), total correlation spectroscopy (TOCSY), and Nuclear Overhauser Effect Spectroscopy (NOESY) and the one-dimensional proton translational diffusion) were performed on a Varian (Palo Alto, CA) INOVA-600 spectrometer using an H cryoprobe at 7°C as previously described (6). Briefly, for each experiment, $Cx43L2_{H142E}$ was dissolved in 0.3 ml of a 10:1 phosphate buffer saline (PBS) buffer/D_2O solution at a final concentration of 0.8 mM. The DQF-COSY, TOCSY, and NOESY experiments were acquired with 1024 complex t2 points and 512 complex t1 points. Mixing times of 50, 150, and 300 ms were used for the NOESY spectra, and a mixing time of 80 ms was used for the TOCSY spectra. Water suppression was achieved by using WATERGATE. Translation diffusion coefficients were measured by a water-sLED experiment which includes water-selective pulses to suppress the intense solvent signal, combined

with an additional interval (longitudinal eddy current delay) that allows the transient perturbations to disappear. A total of 128 scans was collected into a 64-K data block using a sweep width of 8510 Hz. Proton chemical shifts were referenced directly to the water. $Cx43L2_{H142E}$ carbon α and β chemical shifts were analyzed utilizing the natural abundance of ^{13}C in a $^{1}H^{13}C$ HSQC. The $^{1}H^{13}C$ HSQC data were acquired with 1024 complex t2 points and 160 complex t1 points. Spectral widths of proton and carbon resonances were 10,000 and 21,118 Hz, respectively. The number of scan per t1 was 256.

RESULTS

Voltage dependence of H142 mutants

Previous studies have shown that truncation of the CT domain (hence elimination of the putative gating particle) is associated with the loss of fast voltage gating (3). Given the previous demonstration of an association between Cx43CT and the L2 region of Cx43 (6), we assessed whether L2 mutations could also affect voltage gating. Histidine at position 142 (H142) was the focus of these studies, given previous observations showing that this residue is of critical importance for the structural preservation of the region (6). The differences of voltage gating imposed by the H142 mutations were quantified in terms of kinetic properties and steady-state G_j/V_j relationships by forming hybrid junctions comprised of wild-type and mutated hemichannels in the system of *Xenopus* oocyte pairs. Results were compared to those obtained from homologous wild-type Cx43 channels. As shown by the top traces in Fig. 1 *A*, junctional currents flowing through homomeric wild-type channels decreased in response to transjunctional voltage gradients >40 mV (positive or negative), with progressively larger and faster reductions at larger V_js. I_j inactivation in homologous wild-type channels

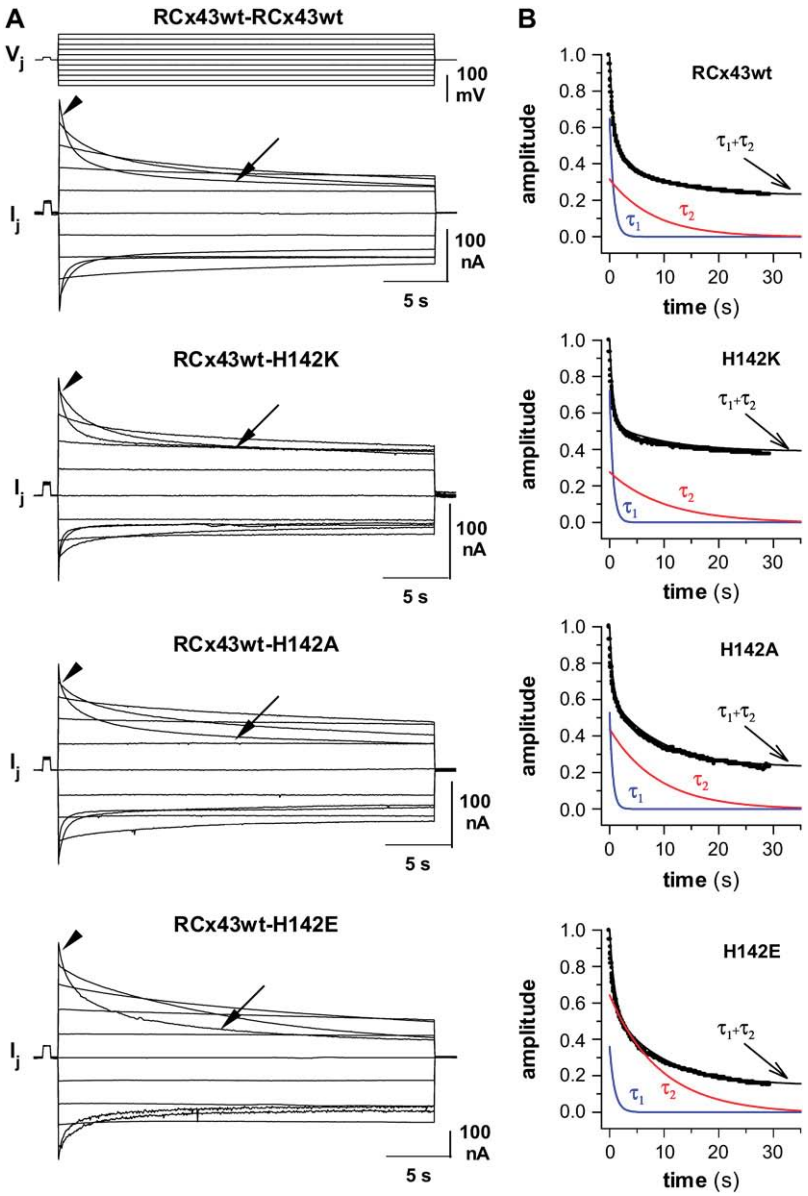

FIGURE 1 Voltage gating of H142 mutants. Differences of voltage gating imposed by the H142 mutations were analyzed in *Xenopus* oocyte pairs by forming hybrid junctions composed of wild-type and mutated hemichannels and homotypic wild-type junctions as control. (*A*) Sample records of junctional currents (I_j) evoked by V_j pulses of ±100 mV in 20-mV increments and of 30-s duration. Positive and negative V_j polarities are defined as relative depolarization and hyperpolarization of the cell expressing the wild-type hemichannels, which induced upward and downward I_js, respectively. Junctional currents of homotypic wild-type channels decreased in response to positive and negative $V_j > 40$ mV, with progressively greater and faster reductions at larger V_js. The I_j decays showed an initial closing of large amplitude and fast kinetics (*arrowhead*) and a second component of smaller amplitude with a slower time course observable for longer pulses (*arrow*). Note that the gating behavior attributable to H142A and H142E hemichannels (i.e., the outward currents) showed, respectively, a mild and pronounced reduction of the fast component of junctional currents (*arrowhead*) and a progressively larger slow I_j inactivation (*arrow*). (*B*) Kinetic properties. The current decays induced for $V_j = +100$ mV in *A* were well fitted by biexponential relations ($\tau_1 + \tau_2$). For comparison, the relative amplitude of fast (τ_1, in *blue*) and slow (τ_2, in *red*) inactivations are represented. The fast component of inactivation was significantly more prominent than the slow component for wild-type and H142K currents, whereas both components were of similar amplitude for H142A and, for H142E, the slow inactivation predominated. Mean values of time constants (mean ± SE) were $\tau_1 = 417 \pm 182$ ms and $\tau_2 = 8.7 \pm 1.3$ s for wild-type, $\tau_1 = 337 \pm 253$ ms and $\tau_2 = 10.8 \pm 1.8$ s for H142K, $\tau_1 = 534 \pm 325$ ms and $\tau_2 = 8.1 \pm 2.1$ s for H142A, and $\tau_1 = 643 \pm 271$ ms and $\tau_2 = 7.6 \pm 1.9$ s for H142E.

was best described as the sum of two exponential functions (see Fig. 1 *B*, *top*). The first component (*blue trace* in Fig. 1 *B*) was of larger relative magnitude and faster kinetics than the second component of inactivation (*red trace* in Fig. 1 *B*). On average, the corresponding time constants for currents elicited by +100 mV V_j pulses were 417 ± 182 ms (τ_1) and 8.7 ± 1.3 s (τ_2) ($N = 6$) with a ratio of amplitudes between the fast and slow components of threefold. Note that, as previously reported (3,11), the time course of current decay and the steady-state G_j/V_j relationships were somewhat asymmetrical depending on the polarity of V_j (see also Fig. 2 *B*).

The formation of hybrid junctions comprised of wild-type and mutated hemichannels allowed us to characterize the effect of H142 substitutions on Cx43 voltage gating. Currents closing for relative negativities on the cytoplasmic side of H142A and H142E clearly showed a reduction in the amplitude of the fast component when compared to that observed in Cx43WT for the same V_j polarity. The effect was more pronounced in the case of H142E but observable in the H142A mutation (see Fig. 1). Indeed, kinetic analysis of the currents elicited by +100 mV V_j pulses showed that the time course of inactivation of H142E currents was best described by a double exponential but, in contrast to the behavior of wild-type currents, in this case the slow component was the one with the largest relative magnitude (see *bottom plot* of Fig. 1 *B*).

It has been previously reported that the contribution of the fast component to the time course of current inactivation is dependent on V_j (3). A similar result was observed for all H142 mutations tested. Moreover, as shown in Fig. 2 *A*, the ratio of magnitudes of the slow versus fast components (ratio A_{slow}/A_{fast}) was higher for H142E and, to a lesser degree, for H142A than for wild-type channels at all voltages tested. These changes in kinetics caused a shift of steady-state G_j/V_j relationships toward lower voltages. As shown in Fig. 2 *B*, relative negativity on the H142E side was associated with a decrease in the junctional conductance measured at steady-state (G_{jss}), for V_j values of 60, 80, and 100 mV. A similar though less drastic reduction was observed in the case of H142A. The minimum G_j (G_{jmin}) value of Boltzmann fits decreased from 0.24 in the wild-type to 0.13 and 0.16 for H142E and H142A hemichannels, respectively. The region of the G_j/V_j curve attributable to H142K hemichannels did not diverge significantly from that of Cx43WT. The G_j/V_j behavior of wild-type hemichannels in the hybrid junctions overlapped with that of their homomeric wild-type junctions, indicating that the characteristics of voltage gating were little affected by its association with mutant hemichannels and that the fast and slow V_j gates of both mutant and wild-type hemichannels closed for the relative negativity of V_j (Figs. 1, *A* and *B*, and 2 *B*).

Effect of H142 mutants on Cx43 channel properties

Mutation H142E caused an important reduction in the amplitude of the fast component of current inactivation. This was reminiscent of what we observed after truncation of the CT domain of Cx43 (3). In that case, single channel analysis demonstrated that the loss of fast voltage gating coincided

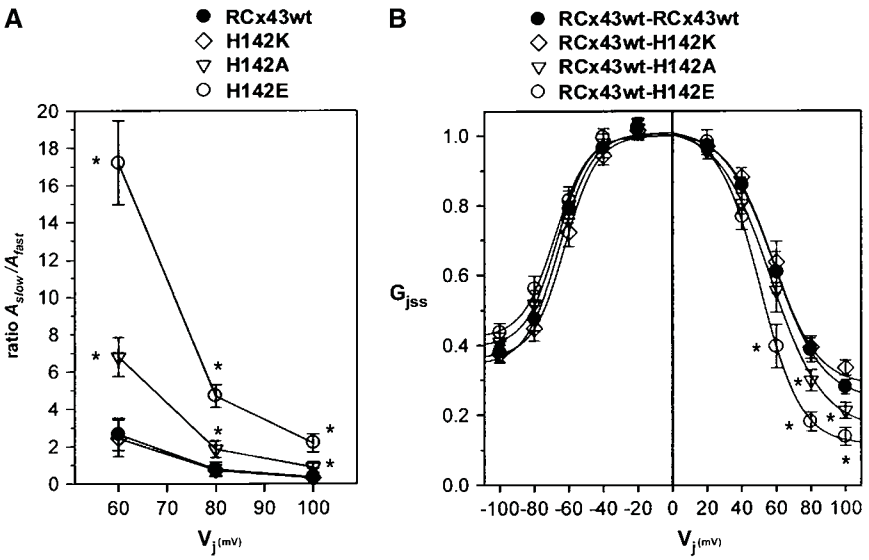

FIGURE 2 Ratio of amplitudes between the slow and fast components of inactivation (*A*) and of the steady-state G_j values versus voltage (*B*) of hybrid wild-type-H142 mutant junctions and homomeric wild-type junctions. Positive and negative V_j polarities in hybrid channels are defined as relative depolarization and hyperpolarization of the cell expressing Cx43WT. (*A*) The time course of junctional current decays induced for V_js followed a biexponential relation with a fast and slow component (indicated as τ_1 and τ_2 in Fig. 1 *B*) and the mean ratio of slow/fast amplitudes (mean ± SE) decreased for increasing V_j. Note that the mutation H142E caused a large reduction in the amplitude of fast gating in the whole range of voltage explored. (*B*) Steady-state values of G_j were measured at the end of the 30-s pulses. The averaged G_j/V_j relationships were well described by a single Boltzmann relation for each polarity of V_j. The Boltzmann parameters of homomeric wild-type junction (●) were $G_{jmin} = 0.36$, $A = 0.10$ mV^{-1}, $V_o = -65.7$ mV for negative V_j and $G_{jmin} = 0.24$, $A = 0.07$ mV^{-1}, $V_o = +58.5$ mV for positive V_j; of hybrid RCx43wt-H142K junction (◇) were $G_{jmin} = 0.36$, $A = 0.11$ mV^{-1}, $V_o = -62.3$ mV for negative V_j and $G_{jmin} = 0.29$, $A = 0.08$ mV^{-1}, $V_o = +57.6$ mV for positive V_j; of hybrid RCx43wt-H142A junction (Δ) were $G_{jmin} = 0.42$, $A = 0.11$ mV^{-1}, $V_o = -66.9$ mV for negative V_j and $G_{jmin} = 0.16$, $A = 0.07$ mV^{-1}, $V_o = +56.6$ mV for positive V_j; and of hybrid RCx43wt-H142E junction (○) were $G_{jmin} = 0.42$, $A = 0.11$ mV^{-1}, $V_o = -68.1$ mV for negative V_j and $G_{jmin} = 0.13$, $A = 0.07$ mV^{-1}, $V_o = +51.1$ mV for positive V_j. In *A* and *B*, each point represents mean values (mean ± SE) of six pairs with <5 μS levels of electrical coupling. Asterisks indicate significant differences relative to wild-type (*t*-test, $P < 0.05$).

with a loss of the residual state and a prolongation of the mean open time (MOT) (see (4)). Here we report that similar results were observed in the case of the H142E mutation. We have analyzed the behavior of unitary currents from homologous H142E channels and compared it with that of wild-type. Fig. 3 shows the results. A single channel trace obtained from a pair of N2a cells expressing homologous Cx43 wild-type channels is shown on the top of Fig. 3 *A*. V_j was 60 mV. An all-points histogram is shown at the right of the trace. Transitions between three states—closed (C), open (O), and residual (r)—are apparent. An all-events histogram, generated by measuring the amplitude of the current transitions between states, is presented in the bottom panel. The data are best described by two Gaussian functions ($N = 5$, $n = 383$; where N is the number of cell pairs and n represents the number of events): one, centered at 80.7 pS, results from the transitions occurring between open and residual states (O-R). The other, centered at 104.5 pS, is consequent to the measurement of transitions between the open and closed states (O-C).

These results are consistent with those extensively described in the literature (4,5,7,12). As an estimate of the fraction of transitions that would be related to fast gating, we calculated the integral of the O-C Gaussian function and divided it by the amplitude of the integral of the O-R function. The resulting ratio was 1.73. Similar calculations from recordings of H142K and H142A channels yielded ratios of 1.26 and 4.43, respectively. This trend correlated well with that obtained from the measurements of the amplitude of the fast and slow components of inactivation at time zero (see Fig. 2 *A*). Indeed, in both cases, the ratio decreased slightly consequent to the H142K mutation, and increased significantly when the same residue was substituted with alanine. Furthermore, in contrast to what was observed in wild-type channels, H142E channel transitions were characterized by the loss of the residual state (Fig. 3 *B*, *top*), and the resulting all-events histogram, depicted in the bottom panel of Fig. 3 *B*, showed a single Gaussian function in the 75–125 pS range (mean value 105.7 pS; $N = 4$, $n = 339$). Data from wild-type channels are shown by the superimposed red dotted line, for comparison.

Additional, very sporadic events of low amplitude were observed, yielding a small cluster of events centered around 50 pS. Moreover, in contrast with the wild-type channel, which showed short residence times in the open state, H142E channels showed a significant prolongation of the MOT. A quantitative analysis is presented in Fig. 4. Panels *A–E* depict the histograms of dwell open time recorded from wild-type, M257 (i.e., a Cx43 mutant lacking most of the CT domain; see (4)), and mutants H142E, H142K, and H142A, respectively. The plots illustrate that MOT for H142E (2.167 ± 0.148 s (mean ± SE); $N = 7$, $n = 276$; see Fig. 4 *C*) was significantly prolonged when compared to that of Cx43WT (0.137 ± 0.026 s; $N = 4$, $n = 148$; Fig. 4 *A*; see also (4)) and similar to (or even longer than) that of M257 (1.604 ± 0.150 s; $N = 3$, $n = 194$; Fig. 4 *B*; see also (4)). In contrast, MOT for H142K channels was similar to that of wild-type (0.173 ± 0.010 s; $N = 5$, $n = 450$; see Fig. 4 *D*), and a slight prolongation was observed for the case of H142A mutant

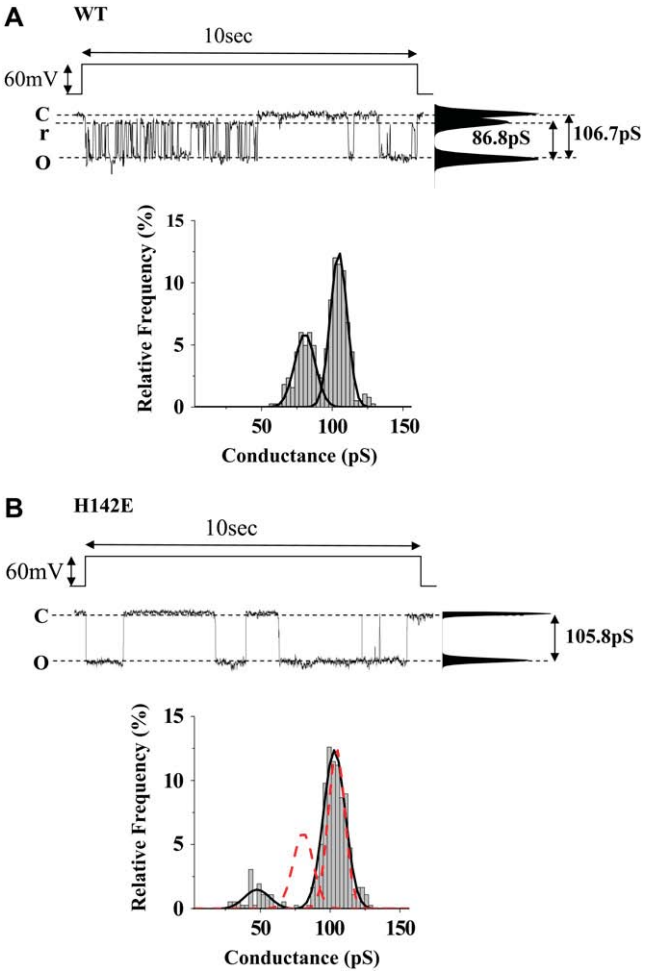

FIGURE 3 Single channel activity recorded from Cx43-transfected N2a cell pairs. (*A*) Top: recording of gap junction channel activity obtained from N2a cells expressing wild-type Cx43. All-points histogram shown at the right. Dotted lines represent current levels for the open (O), closed (C), and residual (r) states. Pulse duration: 10 s. Transjunctional voltage: +60 mV. Pulse applied every 20 s. Bottom: Histogram of amplitude of conductance transitions recorded from Cx43 wild-type channels. The histogram was best described by two Gaussian functions, centered at 80.7 pS and 104.5 pS, corresponding to the transitions between open and residual and open and closed states, respectively ($N = 5$, $n = 383$). Data as in Shibayama et al. (22). (*B*) Top: Junctional current recording obtained from a pair of N2a cells expressing mutant H142E. Only open and closed states were apparent. Bottom: Histogram of amplitude of conductance transitions obtained from H142E-expressing cells. The red dotted line depicts the position of the Gaussian functions describing the histogram obtained from wild-type channels (data in *panel A*). The cluster of data points corresponding to the residual open transitions in wild-type channels was noticeably absent after the H142E mutation. The histogram was centered at 105.7 pS ($N = 4$, $n = 339$). A small peak at 49.6 pS was formed by very low frequency events ($n = 43$). This peak was not observed in recordings from cells expressing wild-type channels.

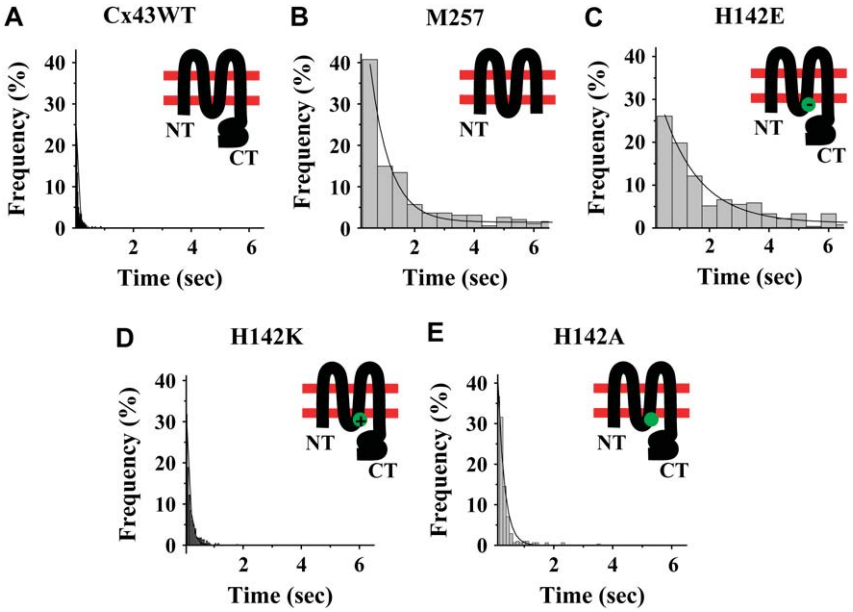

FIGURE 4 Dwell time histograms of channel activity recorded from N2a cells transiently transfected with cDNA coding for Cx43WT (*A*), Cx43M257 (*B*), Cx43H142E (*C*), Cx43H142K (*D*), and Cx43H142A (*E*). H142E showed significantly prolonged open time (MOT = 2.167 ± 0.148 s; $N = 7$, $n = 276$) when compared to Cx43WT (MOT = 0.137 ± 0.026 s; $N = 4$, $n = 148$). MOT recorded from M257 channels was 1.604 ± 0.150 s ($N = 3$, $n = 194$). Panels *D* and *E* depict open time histograms for two additional mutations, H142K (0.173 ± 0.010 s; $N = 5$, $n = 450$) and H142A (0.221 ± 0.010 s; $N = 3$, $n = 331$), respectively. The insets show a diagram of Cx43 topology, indicating the position of amino acid 142 (*green circle*; *panels C–E*).

channels (0.221 ± 0.010 s; $N = 3$, $n = 331$; see Fig. 4 *E*). Channel conductance sublevels in the case of the two latter constructs were unaffected by the mutation. Overall, the single channel analysis yielded results consistent with the notion that mutation H142E caused the loss of the fast gating component of current inactivation.

Binding of Cx43CT to L2: effect of the H142E mutation

The results outlined above are consistent with those previously obtained after truncation of the Cx43CT domain (4). Based on a ''particle-receptor'' model of fast voltage gating (3,4), we used translational diffusion analysis to assess the effect of mutation H142E on the interaction between the CT domain (the presumed ''gating particle''; see (1)) and the putative receptor (region 119–144 of Cx43; dubbed ''L2''; see (6)). Translational diffusion evaluates the mobility of a protein, or a protein complex, within a magnetic field. Given that the diffusion rate of a molecule is dependent on its mass (among other variables), molecular complexes and the proportion of bound versus unbound molecules can be estimated from the rate of mobility of the individual components. Table 1 shows the diffusion rates observed for the H142E peptide in the absence (column labeled ''Cx43L2(H142E)'') and in the presence of Cx43CT (column labeled ''Cx43L2(H142E)/Cx43CT''). Two individual resonance peaks were followed, based on our previous studies on CT-L2 binding (6). To test whether binding in vitro is facilitated by acidification of the solvent (as happens for the ''wild-type'' L2 sequence; see (6)), the experiment was conducted at pH 5.8 and results compared to those obtained at pH 7.5. As shown in the table, a decrease in diffusion rate was observed at low pH, but only after addition of the CT molecule. However, this decrease was significantly less than the one previously observed for the wild-type sequence (see Table III ''Cx43L2/Cx43CT'' in Duffy et al. (6)). Estimation of the proportion of bound versus unbound molecules indicated that, after mutation H142E, only 20% of the L2 molecules were in a complex. In contrast, under the same experimental conditions, 80% of the wild-type L2 sequence was bound to CT (6). These results indicate that the H142E mutation significantly prevented the association between these two protein fragments. As a next step, we determined the effect of the mutation on the secondary structure of the L2 region.

Modification of the secondary structure of L2 consequent to mutation H142E

We have previously defined the secondary structure of the L2 peptide and found it to be organized as two α-helical regions separated by an area of random coil (6). Our previous studies provided the bases for the solution of the structural order of L2 after mutation H142E. The 10 conformers that

TABLE 1 Diffusion experiment in H142E

		Cx43L2(H142E)	Cx43L2(H142E)/Cx43CT
pH 7.5	Peak 1	0.86	0.88
	Peak 2	0.87	0.87
pH 5.8	Peak 1	0.87*	0.79
	Peak 2	0.86	0.76

Translational diffusion of Cx43L2-H142E in the absence (''Cx43L2 (H142E)'') and in the presence of Cx43CT (''Cx43L2(H142E)/Cx43CT''). The decreased diffusion rate after Cx43CT addition (pH 5.8) indicates that ~20% of the molecules are bound. Previous studies showed that ~80% of the Cx43L2-WT peptide binds to Cx43CT (6). The data show that mutation H142E significantly decreased the CT-L2 interaction.
*Diffusion coefficient $\times 10^{-6}$cm^2/s.

best represent the structure of the H142E peptide are presented in Fig. 5 *A*. Only a small area of convergence, covering amino acids 125–128, was found. The lowest energy structures for the wild-type L2 peptide and for the H142E peptide are presented in Fig. 5, *B* and *C*, respectively (amino acids H126 and H142 are indicated in *bold*). Clearly, the H142E mutation disrupted the structural order in the second α-helix (H142E mutation is indicated in *red* in Fig. 5 *C*), leaving only a small, loose helical turn around the H126 region. These results suggest that the reduced ability of peptide H142E (negative charge) to form a molecular complex with CT may be consequent to the disruption in its secondary structure.

DISCUSSION

We have characterized the effect of lysine, alanine, and glutamate substitutions at position H142 on the unitary properties and voltage gating characteristics of Cx43 channels. Our results show that mutation H142E modified the voltage gating behavior of Cx43 in a manner similar to that observed after truncation of the CT domain (see (4)) or after concatenation of aequorin (13) or eGFP to the carboxyl end of Cx43 (14). The data show a concomitant modification in the secondary structure of an H142E-L2 peptide and a significant reduction in the ability of this peptide to bind Cx43CT. Our results indicate that amino acid H142 is part of a Cx43 region involved in the fast voltage gating process, perhaps as a component of a ''receptor'' for the CT domain. Before expanding on the interpretation of our results, some technical aspects of the study need to be considered.

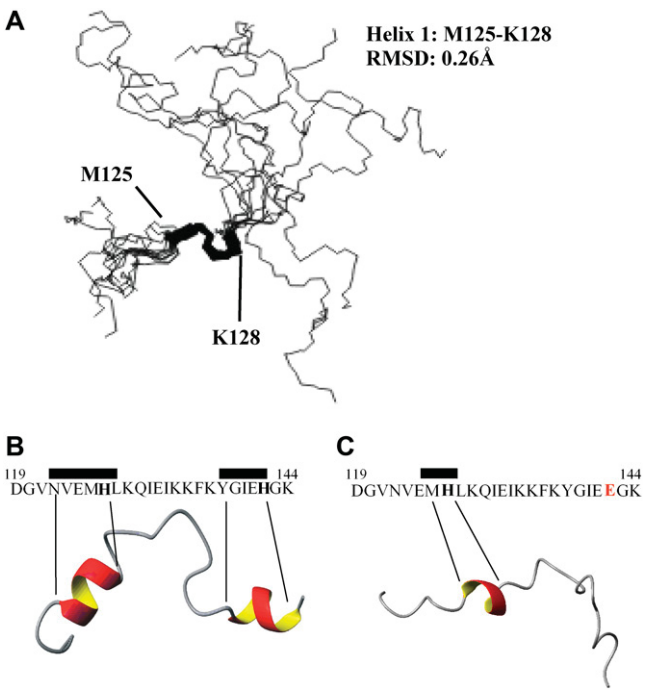

FIGURE 5 Solution structure of Cx43L2-142E (amino acids 119–144). The peptide was diluted in PBS buffer (pH 5.8) and maintained at 7°C. (*A*) Backbone traces of the 10 Cx43L2 mutant peptide (H142E) NMR conformers that best represent the structure are aligned by superimposing the backbone atoms of residues M125–K128 (labeled in *bold*). (*B*) Cx43L2 has two α-helical domains, each containing a histidine residue (positions 126 and 142). (*C*) Cx43L2-H142E. The mutated histidine residue (H142E) was labeled as red. The H142E substitution not only disrupted the folding of the second α-helix, but also influenced the number of residues involved in forming the first α -helix. Helical regions for the lowest energy structure are indicated in color (*red/yellow*). Histidine residues in L2 (H126 and H142) are indicated in bold in panels *B* and *C*.

Technical considerations

Our NMR studies support the contention that the CT binds to the L2 region and that this binding is affected by mutation H142E. Though the results obtained from patch clamp studies are consistent with the in vitro data, we recognize that the behavior of a recombinant protein in solution may differ from that of the native protein in the cellular environment. This concern applies to all in vitro studies, particularly those where protein structures are solved, given the extreme conditions that are often necessary for protein isolation, ordering, and/or crystallization (see, e.g., (6,15–17)). Particularly worth noting in this regard is the fact that the NMR experiments were conducted at a pH of 5.8, given that lowering the pH of the solvent significantly increases the structural order of L2 and the binding affinity of the L2 peptide for CT. Whether the cellular environment facilitates the organization of the structure even at the normal pH of the cell is likely, but remains to be determined.

Our conclusions are supported by experimental data obtained in different systems. A quantitative correlation between the different data sets is limited by the restrictions of each experimental model and by their differences. However, semiquantitative correlates between the data obtained by NMR spectroscopy and the changes in gating behavior at single channel and macroscopic current levels can be noted. Indeed, we estimate that only 20% of L2 molecules carrying the H142E mutation bind to Cx43CT (Table 1); this represents a significant decrease from the 80% reported when studying the wild-type L2 sequence (6). These data are consistent with the large reduction in the amplitude of the fast component of wild-type inactivation from ~75% (wild-type) to ~30% (H142E) at V_j gradients of 100 mV (Fig. 1 *B*), and from ~35% for wild-type to <3% for H142E at moderate V_j gradients (60 mV) (Fig. 2 *A*). The latter, in turn, is also consistent with the virtual disappearance of the residual state observed at the single channel level (Fig. 3 *B*).

Although the quantitative links between one data set and the other are limited, the coincidence of results supports a cohesive hypothesis. Indeed, our data show that the change in time course and voltage dependence of the macroscopic current coincides (albeit in a different cell system) with a significant increase in open time and the loss of the residual state at the single channel level. Similarly, the changes in

single channel and macroscopic currents observed coincide with the loss of the CT-L2 interaction, as seen by translational diffusion, and the loss of the latter coincides with a structural modification in L2 (as shown by NMR). Altogether, these events seem hardly independent from one another. Rather, we speculate that one affects, even if only partially, the other. Although we do not have the ability to make quantitative correlates, this work presents, for the first time to our knowledge, a coincidence of results that together lend support to the hypothesis that the intramolecular interaction of the CT domain with the L2 region is one of the structural features responsible for fast voltage gating of Cx43 channels. Yet, we acknowledge that the findings in one system may only partially explain the results in another, and other factors, undefined by our data, may be involved.

Fast voltage gating and the particle-receptor hypothesis

In 1999, Revilla et al. used the *Xenopus* oocyte system to characterize the voltage gating behavior of a mutant of Cx43 lacking most of the CT domain (mutant ''M257'') (3). Their results showed that CT truncation led to a loss of the fast component of current inactivation, as well as a decrease in G_{jmin}. The authors concluded that CT truncation caused the disappearance of the fast component of Cx43 voltage gating. The single channel behavior of M257 channels expressed in mammalian cells was later assessed by Moreno et al. (4). The data showed that truncation of the CT domain caused the loss of the residual state, a prolongation of MOT, and a decrease in the rate of transition, thus concurring with the notion that the Cx43CT truncation associates with the loss of fast voltage gating. Furthermore, Moreno et al. (4) showed that coexpression of the CT domain as a separate fragment restored the presence of low-conductance states in truncated Cx43 channels. Overall, those results led to the hypothesis that fast voltage gating results, at least in part, from the interaction between the CT domain acting as a gating particle and a separate region of the protein acting as a receptor. This particle-receptor model is similar to that proposed by us for chemical gating of Cx43 (6,7,15).

Separate studies aimed at locating the position of the receptor for the chemical gate pointed to a region of the second half of CL contained between amino acids 119 and 144 (region ''L2'' (6)). The possibility that this region may also be involved in fast voltage gating was explored in a previous study (7). A peptide corresponding to the L2 sequence was diluted in the patch pipette solution, and single Cx43 channel events were recorded. The results showed that the presence of the L2 peptide decreased the frequency of transitions into or out of the residual state. The data were consistent with the notion that the L2 region acted as the receptor for the gating particle. Accordingly, the free L2 peptide would bind to the CT and competitively inhibit the interaction of CT with the native receptor. This hypothesis awaited confirmation by site-directed mutagenesis of the pertinent region. However, those experiments were complicated by the fact that deletions within the region yielded nonfunctional channels (8). In this study, we have circumvented that limitation by using point mutations in an amino acid thought to be critical for proper folding (6). Moreover, we have taken advantage of previous knowledge on the secondary structure of L2 and applied a combination of patch clamp and NMR techniques to further show that structural preservation of the L2 region, and its ability to bind CT, coincide with the presence of fast voltage gating. The results presented in this work show a coincidence of results that can be coherently explained under a single hypothesis. Furthermore, the data are consistent with previous evidence from our laboratories (6,7,15) and in general support the idea of fast voltage gating as a particle-receptor interaction involving the association of the CT domain with the L2 region of Cx43.

The G_{jmin} value of 0.13 obtained in the H142E channels is similar to that previously reported for Cx43 channels in which fast voltage gating was eliminated by truncation of the CT domain (3,4) or by in-frame concatenation of aequorin or eGFP proteins to the C-end of Cx43 (13,14). In the particular case of H142E channels, we speculate that the junctional current at steady-state may be the result of the prolonged open time and perhaps a less stable closed state consequent to the H142E mutation. Indeed, in Fig. 4 *C*, we show that the open time for H142E channels is significantly prolonged, with some openings lasting as long as 10 s. As such, these openings could provide a lingering junctional current even during long voltage pulses. In addition, during our recording of H142E channels, we occasionally observed multiple channel openings occurring late in the voltage step. It was not possible to properly measure open probability under our recording conditions, given the presence of octanol in the recording solution. Yet, as a preliminary assessment, we determined the fraction of time in which the channel was found in the open state during the last second of the 10-s voltage pulse. Data were collected from cells expressing wild-type (100 voltage steps analyzed from four cell pairs) or H142E channels (161 voltage steps analyzed from four cell pairs). Our results showed that the percentage of time that the channel dwelled in the open state during the last second of recording increased, from 6.2% for the wild-type to 50.8% for H142E channels. Overall, our data are consistent with the idea that the H142E mutation renders the closed state nonabsorbing, since the impairment in the CT-L2 interaction could allow for the channel to reopen (or open for the first time) even in the presence of transjunctional voltage. As such, a late channel activity may contribute to the junctional current recorded at steady state. Interestingly, prolonged open time and a nonabsorbing inactivated state have been shown to be responsible for the persistent plateau of sodium inward current observed after some clinically relevant mutations (18).

It is important to note that MOT recorded from H142E channels was longer than that observed from cells expressing M257. These results suggest that H142E may have also affected the properties of the slow gate, perhaps as an indirect consequence of the overall structural modification caused by the mutation. However, the opposite hypothesis (i.e., that the truncation of CT may cause a shortening of the MOT corresponding to the slow gate) is also possible. Future experiments will be directed at addressing these possibilities. The vast majority of single channel events recorded from H142E-expressing cells clustered around one main unitary conductance. However, very occasionally, low-conductance events were recorded (43 out of a total of 339 events; see Fig. 3 *B*). These channels were not recorded from cells expressing the wild-type construct, thus suggesting that an alternative (yet rare) state could be present after the H142 mutation. However, the possibility that those channels may result from the expression of other connexin protein, endogenous to the N2a cell, though unlikely, cannot be completely discarded.

It is interesting to note that the mutation that effectively prevented the residual state was the substitution of a basic residue for the acidic counterpart (H to E). One possible explanation for this result is that the interaction between the CT domain and the L2 region is, at least in part, electrostatic; in that case, H142K would be a relatively conserved mutation, thus explaining the similarity between the results obtained from H142K and those obtained from the wild-type construct (Figs. 1, 2, and 4). Yet, our NMR results show that the H to E substitution caused a significant disruption of the secondary structure of L2. It is therefore not possible to discern at this point to which extent the presence of the acidic residue prevented the CT-L2 association by directly disrupting an electrostatic interaction with a corresponding CT region and to which extent the loss of binding is consequent to an overall loss of structural order in the L2 region.

Other domains involved in fast voltage gating

Our studies suggest that the CT domain interacts with the L2 region to maintain the residual state. This interaction, however, is unlikely to be the only conformational rearrangement responsible for the residual state. In fact, the studies conducted in Cx32 channels have suggested that during V_j gating the NT of the connexin molecule interacts with the pore vestibule, effectively narrowing the pore and increasing the charge density in the region (19,20). Interestingly, the recent results of Bukauskas et al. suggest that a similar model applies to the Cx43 channel (21). Our data complement these results and focus on the possible mechanism by which the CT domain participates in this process. In light of the studies of Bukauskas et al. (21), one possibility could be that the CT domain also interacts with the NT. Though this interaction cannot be completely discarded, it seems unlikely given that these domains do not bind to each other in isolation (6). Another possibility is that the CT-L2 interaction stabilizes the structure of the pore vestibule to then accommodate the formation of the N-terminal-mediated ''gating barrier''. Further studies will assess this or other alternative possibilities.

CONCLUSIONS

We have used a multi-disciplinary approach to characterize the structural and functional consequences of the H142E mutation of Cx43. The data are consistent with the hypothesis that a particle (CT)-receptor (L2) interaction is part of the fast voltage gating process of Cx43 channels. A similar process has been proposed for the chemical gating of Cx43 channels. Whether H142E mutation, now known to disrupt voltage gating, would alter the pH sensitivity of the channels remains to be determined. Overall, our results support the hypothesis that fast voltage gating reflects a particle-receptor interaction which may represent a more general mode of gating for Cx43 channels.

The excellent technical assistance of Wanda Coombs, Li Gao, Chris Burrer, and Fang Lu is very much appreciated.

This study was supported by National Institutes of Health grants GM057691, GM072631, HL080602, and HL39707, by American Heart Association grant AHA 0560050Z, and by ''Ministerio de Educación y Ciencia'' grant SAF2005-03414 to L.C.B.

REFERENCES

1. Morley, G. E., S. M. Taffet, and M. Delmar. 1996. Intramolecular interactions mediate pH regulation of connexin43 channels. *Biophys. J.* 70:1294–1302.
2. Homma, N., J. L. Alvarado, W. Coombs, K. Stergiopoulos, S. M. Taffet, A. F. Lau, and M. Delmar. 1998. A particle-receptor model for the insulin-induced closure of connexin43 channels. *Circ. Res.* 83: 27–32.
3. Revilla, A., C. Castro, and L. C. Barrio. 1999. Molecular dissection of transjunctional voltage dependence in the connexin-32 and connexin-43 junctions. *Biophys. J.* 77:1374–1383.
4. Moreno, A. P., M. Chanson, S. Elenes, J. Anumonwo, I. Scerri, H. Gu, S. M. Taffet, and M. Delmar. 2002. Role of the carboxyl terminal of connexin43 in transjunctional fast voltage gating. *Circ. Res.* 90: 450–457.
5. Moreno, A. P., M. B. Rook, G. I. Fishman, and D. C. Spray. 1994. Gap junction channels: distinct voltage-sensitive and -insensitive conductance states. *Biophys. J.* 67:113–119.
6. Duffy, H. S., P. L. Sorgen, M. E. Girvin, P. O'Donnell, W. Coombs, S. M. Taffet, M. Delmar, and D. C. Spray. 2002. pH-dependent intramolecular binding and structure involving Cx43 cytoplasmic domains. *J. Biol. Chem.* 277:36706–36714.
7. Seki, A., H. S. Duffy, W. Coombs, D. C. Spray, S. M. Taffet, and M. Delmar. 2004. Modifications in the biophysical properties of connexin43 channels by a peptide of the cytoplasmic loop region. *Circ. Res.* 95:e22–e28.
8. Seki, A., W. Coombs, S. M. Taffet, and M. Delmar. 2004. Loss of electrical communication, but not plaque formation, after mutations in the cytoplasmic loop of connexin43. *Heart Rhythm.* 1:227–233.
9. Barrio, L. C., T. Suchyna, T. Bargiello, L. X. Xu, R. S. Roginski, M. V. Bennett, and B. J. Nicholson. 1991. Gap junctions formed by connexins 26 and 32 alone and in combination are differently affected by applied voltage. *Proc. Natl. Acad. Sci. USA.* 88:8410–8414.

10. Spray, D. C., A. L. Harris, and M. V. Bennett. 1981. Equilibrium properties of a voltage-dependent junctional conductance. *J. Gen. Physiol.* 77:77–93.

11. Banach, K., and R. Weingart. 1996. Connexin43 gap junctions exhibit asymmetrical gating properties. *Pflugers Arch.* 431:775–785.

12. Anumonwo, J. M., S. M. Taffet, H. Gu, M. Chanson, A. P. Moreno, and M. Delmar. 2001. The carboxyl terminal domain regulates the unitary conductance and voltage dependence of connexin40 gap junction channels. *Circ. Res.* 88:666–673.

13. Martin, P. E., C. H. George, C. Castro, J. M. Kendall, J. Capel, A. K. Campbell, A. Revilla, L. C. Barrio, and W. H. Evans. 1998. Assembly of chimeric connexin-aequorin proteins into functional gap junction channels. Reporting intracellular and plasma membrane calcium environments. *J. Biol. Chem.* 273:1719–1726.

14. Bukauskas, F. F., A. Bukauskiene, M. V. Bennett, and V. K. Verselis. 2001. Gating properties of gap junction channels assembled from connexin43 and connexin43 fused with green fluorescent protein. *Biophys. J.* 81:137–152.

15. Sorgen, P. L., H. S. Duffy, S. M. Cahill, W. Coombs, D. C. Spray, M. Delmar, and M. E. Girvin. 2002. Sequence-specific resonance assignment of the carboxyl terminal domain of connexin43. *J. Biomol. NMR.* 23:245–246.

16. Sorgen, P. L., S. M. Cahill, R. D. Krueger-Koplin, S. T. Krueger-Koplin, C. C. Schenck, and M. E. Girvin. 2002. Structure of the Rhodobacter sphaeroides light-harvesting 1 beta subunit in detergent micelles. *Biochemistry.* 41:31–41.

17. Krueger-Koplin, R. D., P. L. Sorgen, S. T. Krueger-Koplin, I. O. Rivera-Torres, S. M. Cahill, D. B. Hicks, L. Grinius, T. A. Krulwich, and M. E. Girvin. 2004. An evaluation of detergents for NMR structural studies of membrane proteins. *J. Biomol. NMR.* 28:43–57.

18. Kambouris, N. G., H. B. Nuss, D. C. Johns, G. F. Tomaselli, E. Marban, and J. R. Balser. 1998. Phenotypic characterization of a novel long-QT syndrome mutation (R1623Q) in the cardiac sodium channel. *Circulation.* 97:640–644.

19. Ri, Y., J. A. Ballesteros, C. K. Abrams, S. Oh, V. K. Verselis, H. Weinstein, and T. A. Bargiello. 1999. The role of a conserved proline residue in mediating conformational changes associated with voltage gating of Cx32 gap junctions. *Biophys. J.* 76:2887–2898.

20. Purnick, P. E., D. C. Benjamin, V. K. Verselis, T. A. Bargiello, and T. L. Dowd. 2000. Structure of the amino terminus of a gap junction protein. *Arch. Biochem. Biophys.* 381:181–190.

21. Bukauskas, F. F., A. Bukauskiene, and V. K. Verselis. 2002. Conductance and permeability of the residual state of connexin43 gap junction channels. *J. Gen. Physiol.* 119:171–185.

22. Shibayama, J., R. Lewandowski, F. Kieken, W. Coombs, S. Shah, P. L. Sorgen, S. M. Taffet, and M. Delmar. 2006. Identification of a novel peptide that interferes with the chemical regulation of connexin43. *Circ. Res.* 98: 1365–1372.